

Supporting Information

Immobilised Electrocatalysts: Nafion Particles Doped with Ruthenium (II)

Tris(2,2'-bipyridyl)

Haiying Yang ^{a,b}, Xiuting Li ^b, Christopher Batchelor-McAuley ^b, Stanislav V. Sokolov ^b,

Enno Kätelhön ^b, and Richard G. Compton ^{b*}

^a Department of Chemistry, Yuncheng University, Yuncheng, 044000, P. R. China

^b Department of Chemistry, Physical & Theoretical Chemistry Laboratory, Oxford University, Oxford, OX1 3QZ, United Kingdom

Corresponding Author

*Correspondence to: Richard.compton@chem.ox.ac.uk

Telephone number: +44(0) 1865 275957

Table of contents:

Section 1: Selective overview of some of the reports in the literature on the use of Nafion as an electrolyte membrane, proton transportation and catalytic support.

Section 2: Dependence of the oxidative current on the concentration of $\text{Ru}(\text{bpy})_3^{2+}$ used for the preparation of Ru-Nafion particles.

Section 3: Characterization of Nafion particles by SEM and UV-Vis spectroscopy.

Section 4: Estimation of the amount of $\text{Ru}(\text{bpy})_3^{2+}$ doped into one single Ru-Nafion particle.

Section 5: Dependence of the oxidative peak current on the amount of Ru-Nafion particles in dropcast experiment.

Section 6: Dependence of the oxidative peak current on the square root of scan rate by drop-casting Ru-Nafion particles on a GC electrode.

Section 7: Estimated of the diffusion coefficient of $\text{Ru}(\text{bpy})_3^{2+}$ in the Nafion particles.

Section 8: Chronoamperometric profiles of Ru-Nafion particles at different potentials in 10 mM PBS (pH 7.4).

Section 9: Cyclic voltammograms recorded at a GC modified with Nafion particles and Ru-Nafion particles in 0 mM and 6 mM $\text{Na}_2\text{C}_2\text{O}_4$ solution.

Section 10: Cyclic voltammograms of 1 mM $\text{Na}_2\text{C}_2\text{O}_4$ solution recorded at a GC electrode modified with and without Nafion particles.

Section 11: Cyclic voltammograms of 1 mM $\text{Na}_2\text{C}_2\text{O}_4$ solution recorded at a micro carbon wire electrode and a macro GC electrode.

Section 12: Comparison of the dependence of the oxidative charge on the duration time of spikes of Ru-Nafion particles in the concentration of sodium oxalate from 0 to 6 mM.

Section 13: Schematic illustration of the formation of Nafion particles with the re-precipitation method.

Section 1:

Table S1 Some reports of applications of Nafion in the sustainable energy technologies (fuel cells, batteries and solar cells) and in electrochemical sensors and biosensors are listed as follows.

Fuel cells:

Nafion	Function	References
Graphene/Nafion	Proton transportation	Proton transport through one-atom-thick crystals. <i>Nature</i> , 2016, 516, 227-230.
SWCNT ^a /Nafion	Proton transportation	Polymer electrolyte fuel cells using Nafion-based composite membranes with functionalized carbon nanotubes. <i>Angew. Chem., Int. Ed.</i> , 2008, 47, 2653-2656.
Nafion nanofiber	Proton transportation	Super proton conductive high-purity Nafion nanofibers. <i>Nano Lett.</i> , 2010, 10, 3785-3790
Nafion/Pt/GC ^b	Proton exchange	Nafion structural phenomena at platinum and carbon interfaces. <i>J. Am. Chem. Soc.</i> , 2009, 131, 18096-18104.
Nafion/poly(1-vinylimidazole)	Proton exchange	Nafion-initiated ATRP of 1-Vinylimidazole for preparation of proton exchange membranes. <i>ACS Appl. Mater. Interfaces</i> , 2016, 8, 11516-11525.
SiO ₂ /Nafion	Proton exchange	An amphiphilic-like fluoroalkyl modified SiO ₂ nanoparticle@Nafion proton exchange membrane with excellent fuel cell performance. <i>Chem. Commun.</i> , 2013, 49, 9639-9641.
Nafion/Graphene oxide/Pt	Ionic exchange	Multifunctional graphene/platinum/ Nafion hybrids via ice templating. <i>J. Am. Chem. Soc.</i> 2011, 133, 6122-6125.
Pt nanoparticles/Nafion	Catalyst support	Nafion®-stabilised Pt/C electrocatalysts with efficient catalyst layer ionomer distribution for proton exchange membrane fuel cells. <i>RSC Adv.</i> , 2012, 2, 8368-8374.

Nafion/Polyaniline nanofiber	Catalyst support	Study of co-electrospun Nafion and polyaniline nanofibers as potential catalyst support for fuel cell electrodes. <i>Electrochimica Acta</i> , 2016,198, 156-164.
Pt/C particles/Nafion	Catalyst layer	Fuel cell catalyst layers: a polymer science perspective. <i>Chem. Mater.</i> 2014, 26, 381-393.

Solar cells or batteries:

Nafion	Function	References
Nafion/Organic polymer	Electrolyte membrane	An aqueous, polymer-based redox-flow battery using non-corrosive, safe, and low-cost materials. <i>Nature</i> , 2015, 527, 78-81.
Nafion/Graphene oxide	Electrolyte membrane	A recast Nafion/graphene oxide composite membrane for advanced vanadium redox flow batteries. <i>RSC Adv.</i> , 2016, 6, 3756-3763.
Ru/TiO ₂ /Nafion	Electrolyte membrane	Solar driven water oxidation by a bioinspired manganese molecular catalyst. <i>J. Am. Chem. Soc.</i> , 2010, 132, 2892-2894.
SiO ₂ /Nafion	Electrolyte membrane	Controlling Nafion structure and properties via wetting interactions. <i>Macromolecules</i> , 2012, 45, 4681-4688.
Si microwire/Nafion	Electrolyte membrane	Tailoring of interfacial mechanical shear strength by surface chemical modification of silicon microwires embedded in Nafion membranes. <i>ACS Nano</i> , 2015, 9, 5143-5153.
Nafion film	Ion exchange	Photoelectrochemistry of photosystem I bound in Nafion, <i>Langmuir</i> 2014, 30, 13650-13655.
Nafion film	Gas transportation	Improving the gas barrier properties of Nafion via thermal annealing: evidence for diffusion through hydrophilic channels and matrix. <i>Macromolecules</i> , 2015, 48, 3303-3309.

Sensors:

Nafion	Function	References
Polymeric porphyrin/Nafion	Electrochemical sensors	Nitric oxide release from a single cell measured in situ by a porphyrinic-based microsensor. <i>Nature</i> , 1992, 358, 676-678.
SWCNT ^a -Nafion	Electrochemical biosensors	Solubilisations of carbon nanotubes by Nafion toward the preparation of amperometric biosensors. <i>J. Am. Chem. Soc.</i> 2003, 125, 2408-2409.
MWCNT ^c /Nafion	Electrochemical sensor	Carbon nanotube-loaded Nafion film electrochemical sensor for metal ions: europium. <i>Anal. Chem.</i> , 2014, 86, 4354-4361.
MWCNT ^c /Nafion/Boron-doped diamond electrode	Electrochemical biosensors	Selective electrochemical detection of ciprofloxacin with a porous Nafion/multiwalled carbon nanotube composite film electrode. <i>ACS Appl. Mater. Interfaces</i> , 2016, 8, 1615-1626.
Reduced graphene oxide/Ag nanoparticles/Nafion	Electrochemical biosensors	Ternary nanohybrid of reduced graphene oxide-Nafion@silver nanoparticles for boosting the sensor performance in non-enzymatic amperometric detection of hydrogen peroxide. <i>Biosens. Bioelectron.</i> , 2017, 87, 1020-1028.
Ru(bpy) ₃ ²⁺ /Nafion/Fe ₃ O ₄	Electrogenerated chemiluminescence sensor	Nafion-stabilized magnetic nanoparticles (Fe ₃ O ₄) for [Ru(bpy) ₃] ²⁺ (bpy = bipyridine) electrogenerated chemiluminescence sensor, <i>Chem. Commun.</i> , 2005, 2966-2968.

Abbreviations:

^a SWCNT is single walled carbon nanotubes.

^b GC is glassy carbon.

^c MWCN is multi walled carbon nanotubes.

Section 2:

Dependence of oxidative current on the concentration of $\text{Ru}(\text{bpy})_3^{2+}$ for the preparation of Ru-Nafion particles.

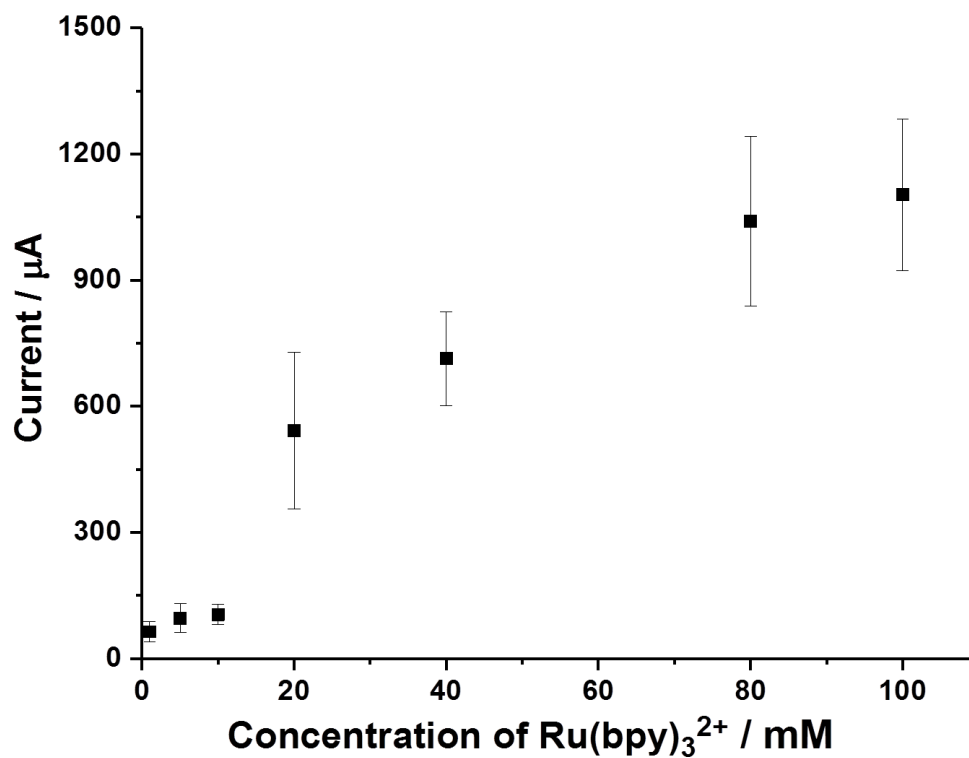


Figure S1. Dependence of peak current on the concentration of $\text{Ru}(\text{bpy})_3^{2+}$ for the preparation of Ru-Nafion particles. Voltammetric oxidative peak current was obtained by drop-casting 1.5×10^8 particles at a GC electrode ($d = 3$ mm) in 10 mM PBS (pH 7.4) containing 0.1 M KCl at the scan rate of 0.1 V s^{-1} .

Section 3:

Characterization of Nafion particles by SEM and UV-Vis spectroscopy.

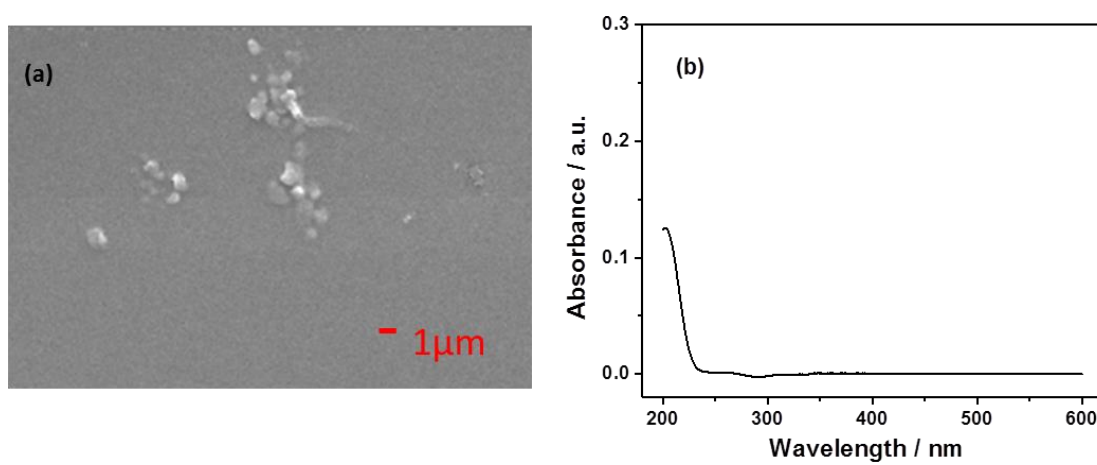


Figure S2. a) SEM image of the Nafion particles. b) UV-Vis spectroscopy of the Nafion particles suspension.

Section 4:

Estimation of the amount of $\text{Ru}(\text{bpy})_3^{2+}$ doped into one single Ru-Nafion particle.

The maximum uptake of Ru(II) onto Nafion can be estimated via measurement of the absorption maximum of $\text{Ru}(\text{bpy})_3^{2+}$ in solution at 454 nm using UV-Vis spectroscopy before and after absorption into the Nafion particles. The absorbance loss relates to the amount of $\text{Ru}(\text{bpy})_3^{2+}$ incorporated in the Ru-Nafion particles. Using the Beer-Lambert law the Ru^{2+} : Nafion ratio can be calculated to be $9.9 \pm 3.3 \times 10^{18}$ Ru ions per gram Nafion using the following expression,

$$N_A \times \left(\frac{A_{\text{before}} - A_{\text{after}}}{\varepsilon l} \right) \times \frac{V}{m_{\text{nafion}}} \quad (1)$$

where ε is the molar extinction coefficient of $\text{Ru}(\text{bpy})_3^{2+}$ with a value of $1.4 \times 10^4 \text{ M}^{-1} \text{ cm}^{-1}$,^[1] l is the optical path of 0.1 cm, A_{before} and A_{after} are the absorbance of $\text{Ru}(\text{bpy})_3^{2+}$ solution before and after the absorption. V is the volume of the $\text{Ru}(\text{bpy})_3^{2+}$ in solution.^[2] The mass of one single particle is $7.7 \times 10^{-13} \text{ g}$ ($m = \frac{\rho 4\pi r^3}{3}$, $r = 0.46 \pm 0.40 \text{ }\mu\text{m}$, $\rho = 1.858 \text{ g cm}^{-3}$).^[3] Thus, the maximum number of Ru(II) molecules doped into a single Nafion particle is $7.6 \pm 4.8 \times 10^6$.

Section 5:

Dependence of the oxidative peak current on the amount of Ru-Nafion particles in the dropcast experiment.

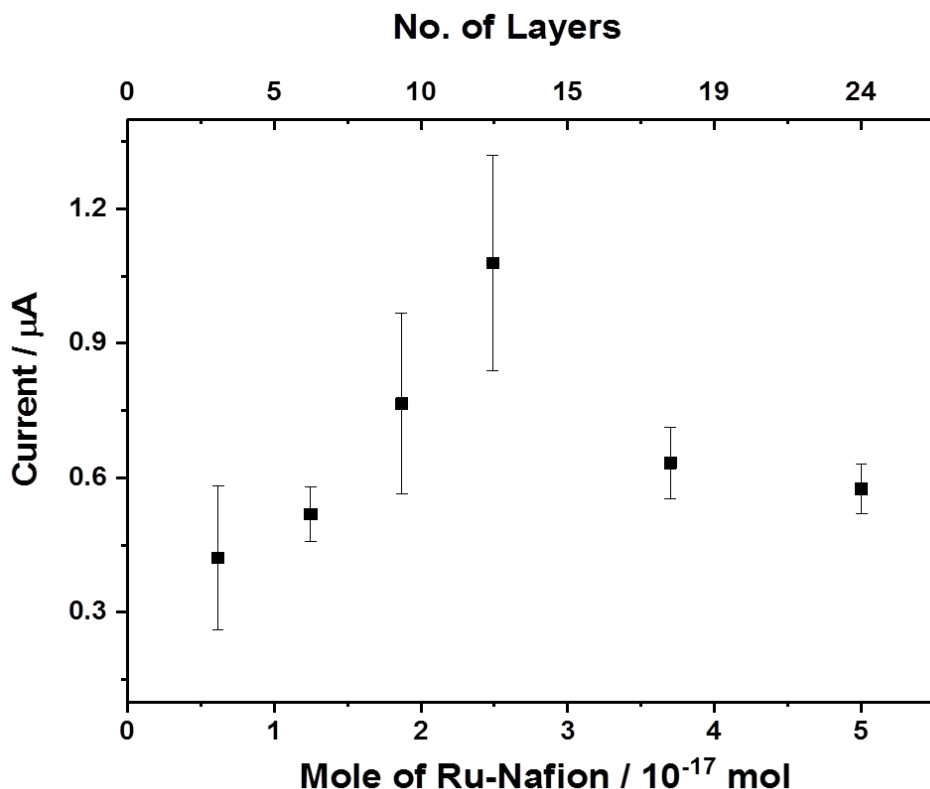


Figure S3. Dependence of the voltammetric oxidative peak current on the amount of Ru-Nafion particles drop-casted on a GC electrode in 10 mM PBS (pH 7.4) containing 0.1 M KCl at the scan rate of 0.1 V s⁻¹. The error bar was obtained from three repeats. The amount of Ru-Nafion particles ranges from 6.2×10^{-18} mol to 5.0×10^{-17} mol equivalent to the number of particles from 3.7×10^6 to 3.0×10^7 .

A GC macroelectrode dropcast with varying amount of Ru-Nafion particles range of 6.2×10^{-18} mol to 5.0×10^{-17} mol was investigated (Figure S3). At the small coverages from 6.2×10^{-18} mol to 2.5×10^{-17} mol, the magnitude of the Ru(bpy)₃²⁺ voltammetric response is found to be roughly constant within error. The thickness of the Ru-Nafion particles coated on the electrode surface was estimated by converting the mass of dropcast material into the average

number of monolayers. Assuming the Ru-Nafion particles is quasi-spherical, and the number of layers ($N_{\text{particles}}$) of particles is calculated based on the following Equation (1):

$$N_{\text{particles}} = \frac{cV}{\frac{A}{\pi r^2} \times \rho \times \frac{4}{3} \pi r^3} = \frac{3cV}{4A\rho r} \quad (1)$$

where c is the concentration of Ru-Nafion particles, V is the dropcast volume, ρ represents the Nafion density in water (1.858 g m^{-3}),^[3] A is the geometric surface area of the electrode, and r is the radius of the particles from SEM analysis. 2.5×10^{-17} mole Ru-Nafion particles casted on a GC electrode corresponding to 14 layers of particles gives the highest oxidation current. It becomes difficult to observe the $\text{Ru}(\text{bpy})_3^{2+}$ oxidation at less than 3 layers, which is likely due to the formation of the tangled and irregular mat of the particles coupled with agglomeration/aggregation at the particles.

Section 6:

Dependence of the oxidative peak current on the square root of scan rate by dropcasting Ru-Nafion particles on a GC electrode.

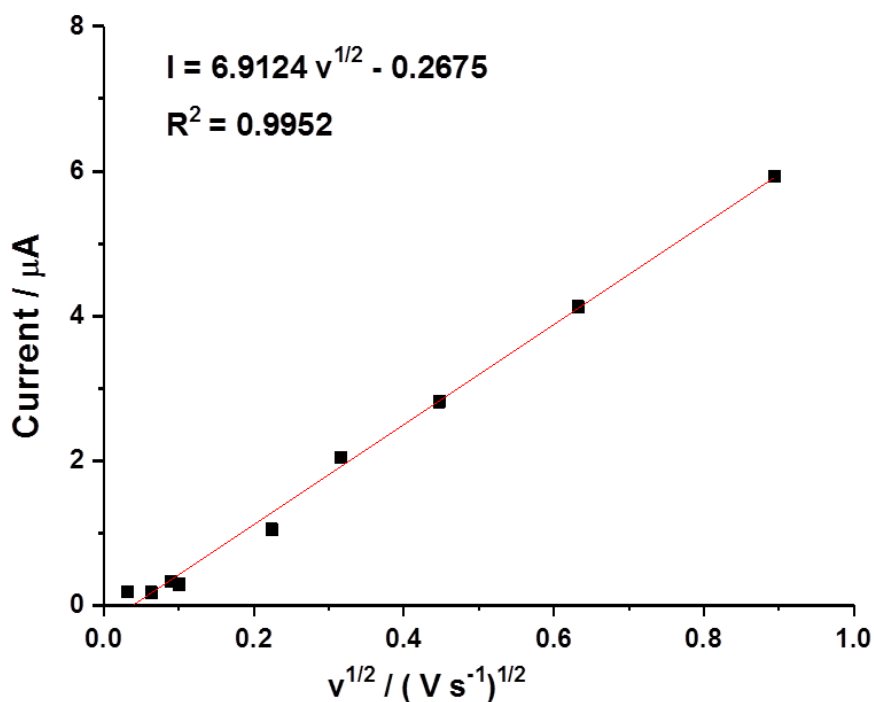


Figure S4. Oxidative peaks current versus square root of scan rates from 0.001, 0.004, 0.008, 0.01, 0.05, 0.1, 0.2, 0.4 and 0.8 V s^{-1} . The current were obtained by drop-casting 1.5×10^8 Ru-Nafion particles on a GC electrode in 10 mM PBS buffer (pH 7.4) with 0.1 M KCl.

Section 7:

Estimation of the diffusion coefficient of $\text{Ru}(\text{bpy})_3^{2+}$ in the Nafion particles.

The oxidative peak current is found to vary linearly with the square root of the scan rate ($I = 6.91 \times 10^{-6} v^{1/2} - 0.2675$, $R^2 = 0.9952$), suggesting that it is a diffusional control process. Then, the diffusion coefficient (D) of $\text{Ru}(\text{bpy})_3^{2+}$ incorporated Nafion particles was estimated according to the Randles-Sevcik equation,

$$I = 2.69 \times 10^5 n^{3/2} A D^{1/2} C_{\text{Ru}} v^{1/2}$$

where n is the transfer electron of 1, D is the diffusion coefficient, C_{Ru} is $\text{Ru}(\text{bpy})_3^{2+}$ incorporated Nafion particles, A is the electrode area ($7.07 \times 10^{-6} \text{ m}^2$), v is the scan rate.

For the concentration of $\text{Ru}(\text{bpy})_3^{2+}$ incorporated Nafion particles can be estimated by the following equation:

$$C_{\text{Ru}} = \frac{n_{\text{Ru}}}{m_{\text{Nafion,tot}} / \rho}$$

n_{Ru} is the moles of $\text{Ru}(\text{bpy})_3^{2+}$ from UV-Vis results, $m_{\text{Nafion,tot}}$ is the mass of Nafion in the particles, ρ is the density of Nafion.^[3] Accordingly C_{Ru} of $3.11 \times 10^{-2} \text{ mol} \cdot \text{dm}^{-3}$ was obtained. The diffusion coefficient is therefore estimated to be $1.4 \times 10^{-10} \text{ cm}^2 \text{ s}^{-1}$ which is consistent with the voltammetric behavior of $\text{Ru}(\text{bpy})_3^{2+}$ in Nafion film.^[4]

Section 8:

Chronoamperometric profiles of Ru-Nafion particles at different potentials in 10 mM PBS (pH 7.4).

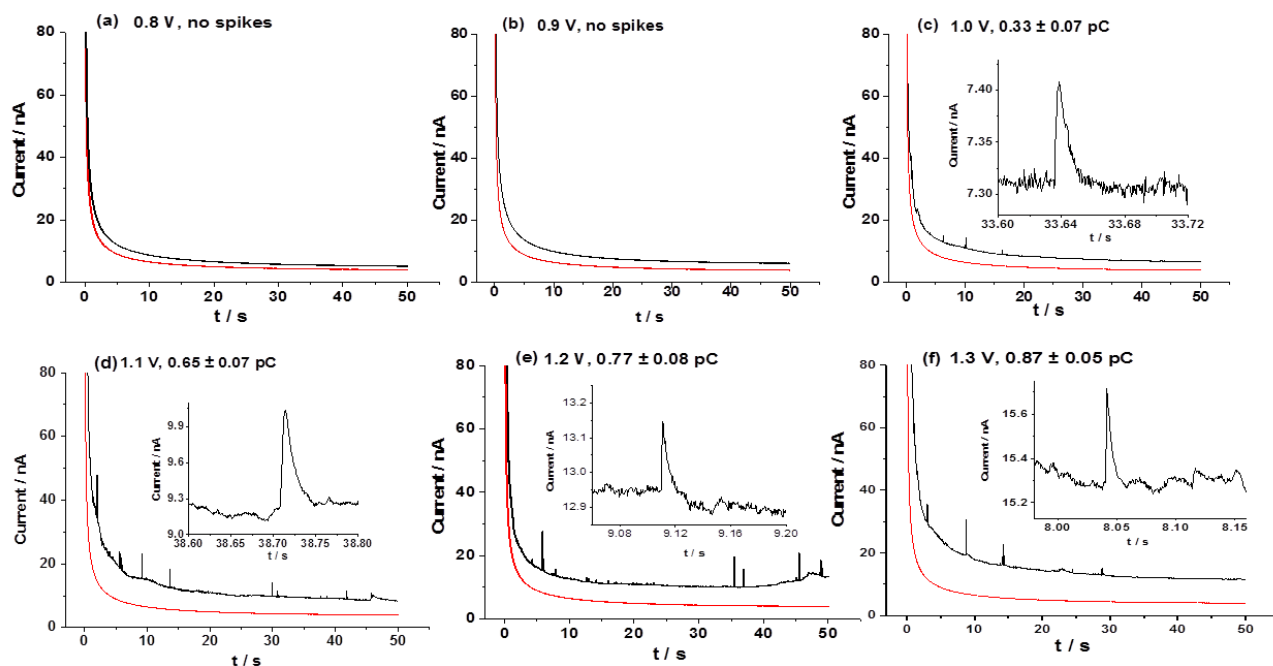


Figure S5. Chronoamperometric profiles showing oxidative faradaic spikes of 2.5×10^{-13} mol \cdot dm $^{-3}$ Ru-Nafion particles in 10 mM PBS buffer (pH 7.4) containing 0.1 M KCl a) 0.8 V, b) 0.9 V, c) 1.0 V, d) 1.1 V, e) 1.2 V and f) 1.3 V (*vs.* SCE). The inset shows the detailed impact spikes.

Section 9:

Cyclic voltammograms recorded at a GC modified with Nafion particles and Ru-Nafion particles in 0 mM and 6 mM $\text{Na}_2\text{C}_2\text{O}_4$ solution.

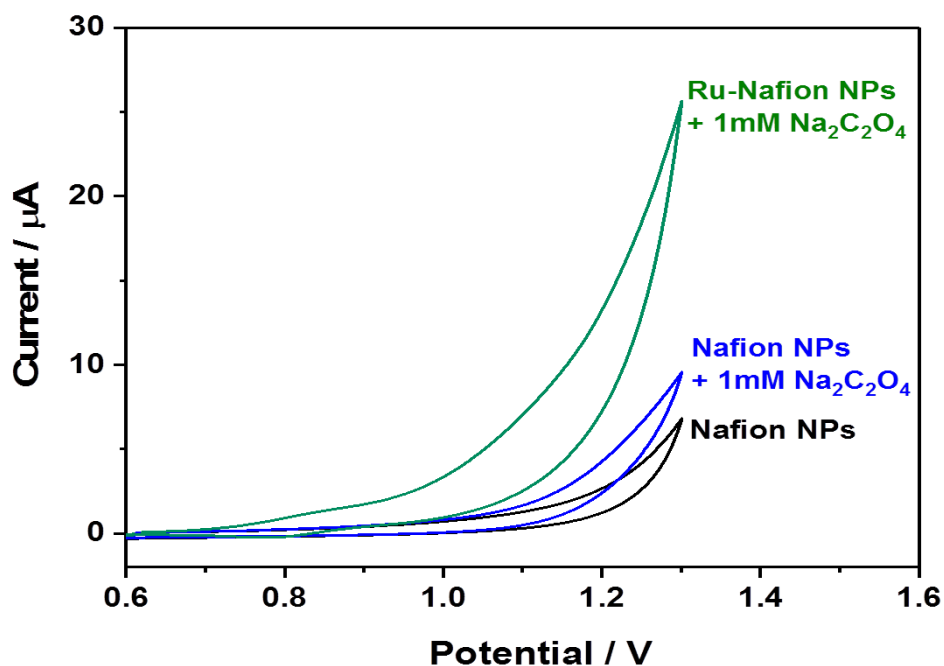


Figure S6. Cyclic voltammograms recorded at a GC electrode modified with 1.5×10^8 Nafion particles in 0 mM $\text{Na}_2\text{C}_2\text{O}_4$ (black curve), 1 mM $\text{Na}_2\text{C}_2\text{O}_4$ (blue curve), and with 1.5×10^8 Ru-Nafion particles in 1 mM $\text{Na}_2\text{C}_2\text{O}_4$ solution (green curve) supported by 10 mM PBS (pH 7.4) containing 0.1 M KCl at a scan rate of 0.1 V s^{-1} .

Section 10:

Cyclic voltammograms of 1 mM $\text{Na}_2\text{C}_2\text{O}_4$ solution recorded at a GC electrode modified with and without Nafion particles.

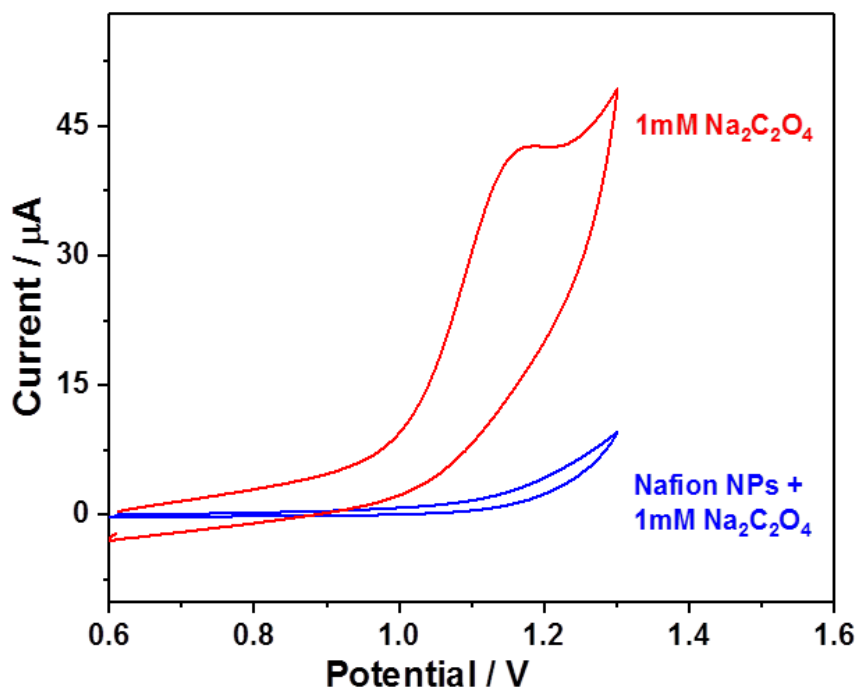


Figure S7. Cyclic voltammograms recorded at a GC electrode modified with (blue curve) and without (red curve) 1.5×10^8 Nafion particles in 1 mM $\text{Na}_2\text{C}_2\text{O}_4$ supported by 10 mM PBS (pH 7.4) containing 0.1 M KCl at a scan rate of 0.1 V s^{-1} .

Section 11:

Cyclic voltammograms of a 1 mM $\text{Na}_2\text{C}_2\text{O}_4$ solution recorded at a micro carbon wire electrode and a macro GC electrode.

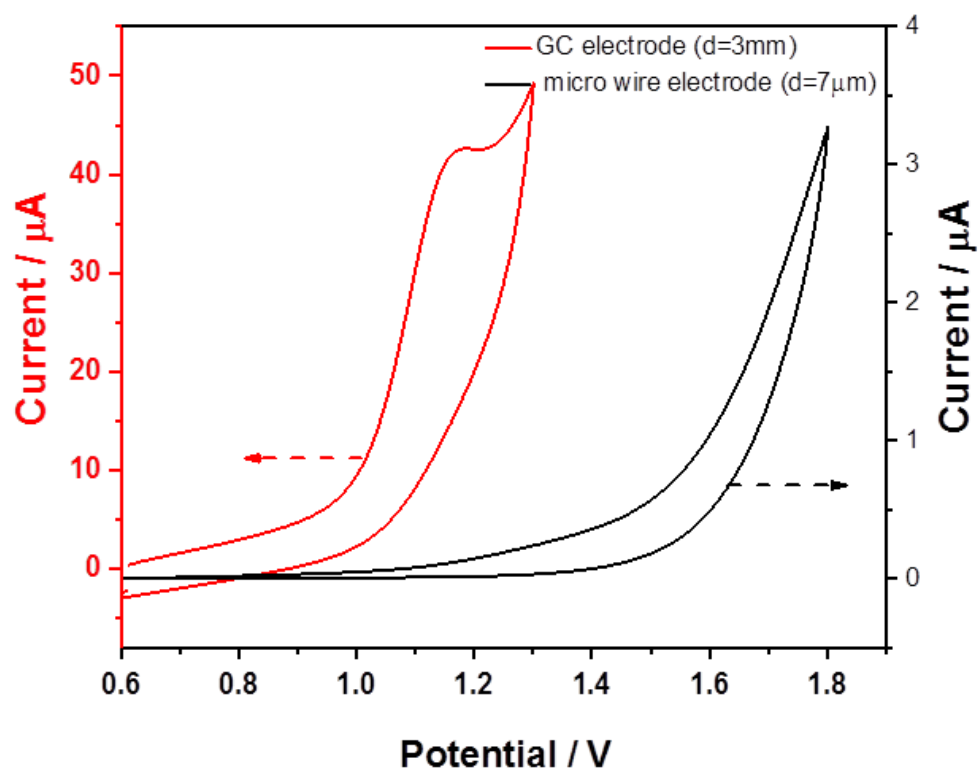


Figure S8. Cyclic voltammograms recorded of 1 mM $\text{Na}_2\text{C}_2\text{O}_4$ solution at a micro carbon wire electrode (black curve) and a macro GC electrode (red curve) in 10 mM PBS (pH 7.4) and 0.1 M KCl. The scan rate is 0.1 V s^{-1} .

Section 12:

Comparison of the dependence of the oxidative charge on the duration time of spikes of Ru-Nafion particles in the concentration of sodium oxalate from 0 to 6 mM.

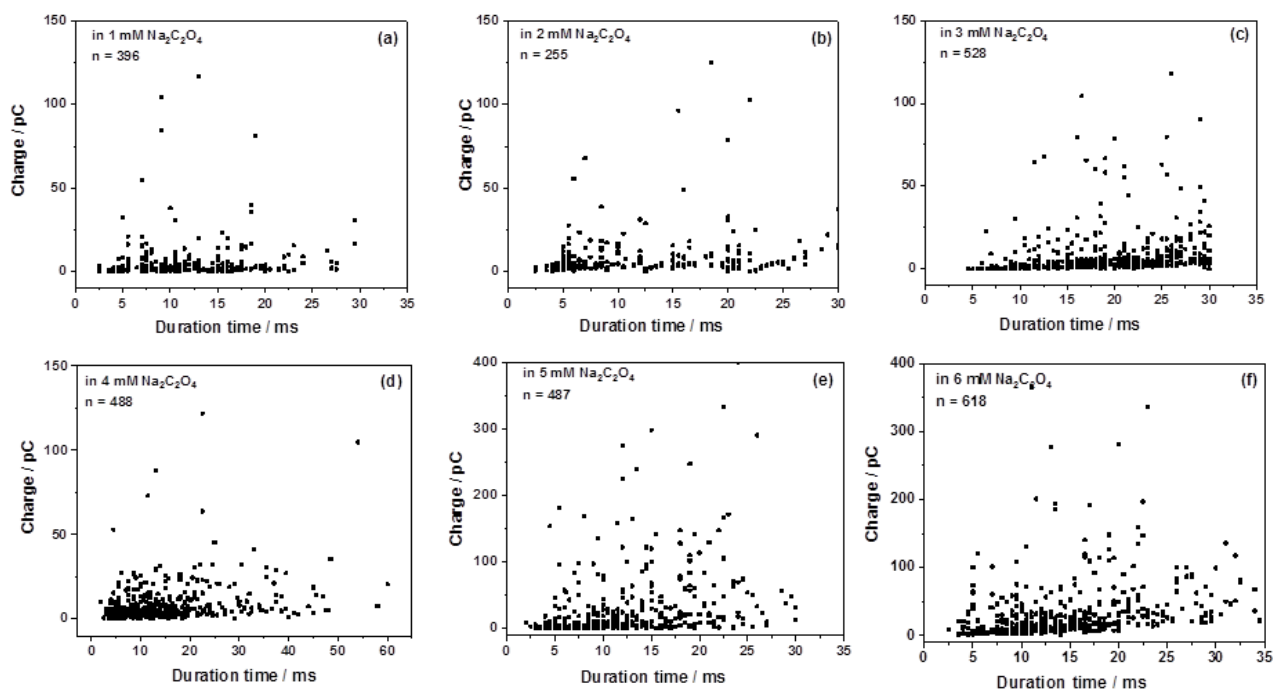
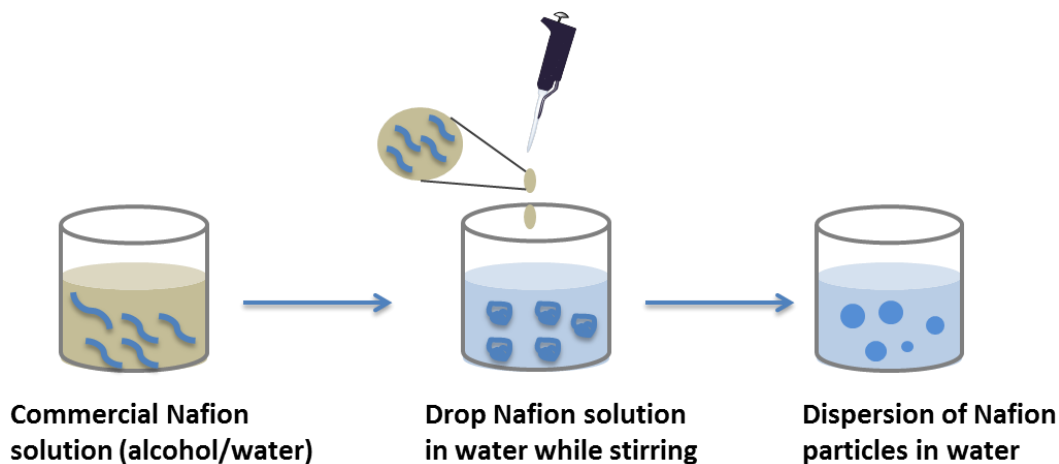


Figure S9. Dependence of the spike charge on the duration time of $2.5 \times 10^{-13} \text{ mol} \cdot \text{dm}^{-3}$ Ru-Nafion particles in 0, 1, 2, 3, 4, 5 and 6 mM $\text{Na}_2\text{C}_2\text{O}_4$ solution (from a to f) in 10 mM PBS (pH 7.4) containing 0.1 M KCl at + 1.1 V vs. SCE, respectively.

Section 13:

Schematic illustration of the formation of Nafion particles with the re-precipitation method.



Scheme S1: Illustration of the formation of Nafion particles with the re-precipitation method.

References and Note

- [1] K. Kalyanasundaram, *Coordin. Chem. Rev.* **1982**, *46*, 159.
- [2] Noting that the absorbance of Ru-Nafion particles was not directly used to calculate the amount of $\text{Ru}(\text{bpy})_3^{2+}$ incorporated in Ru-Nafion particles. This is because the absorbance of $\text{Ru}(\text{bpy})_3^{2+}$ is sensitive to the surrounding environment of the complex cation of Nafion and shows smaller extinction efficient than that in aqueous soltuion, which will lead to inaccurate estimation.
- [3] T. Takamatsu, A. Eisenberg, *J. Appl. Polym. Sci.* **1979**, *24*, 2221.
- [4] D. A. Buttry, F. C. Anson, *J. Am. Chem. Soc.* **1982**, *104*, 4824.